ELSEVIER

Surface Science 507–510 (2002) 700–706

SURFACE SCIENCE

www.elsevier.com/locate/susc

AFM/LFM surface studies of a ternary polymer blend cast on substrates covered by a self-assembled monolayer

P. Cyganik, A. Budkowski *, J. Raczkowska, Z. Postawa

Smoluchowski Institute of Physics, Jagiellonian University, ul. Reymonta 4, 30-059 Kraków, Poland

Abstract

Nanometer films composed of model ternary blend of deuterated polystyrene (dPS), poly(2-vinylpyridine) (PVP) and poly(methyl methacrylate) (PMMA) were studied after spin-coating from a common solvent. Surface undulations and the distribution of phase-separated domains at the surface and in the bulk are closely related as revealed by atomic (AFM) and lateral (LFM) force microscopy. For the first time the chemical sensitivity of LFM is demonstrated for a ternary polymer mixture. In this case PMMA intercalates between dPS and PVP leading to extended interfaces and surface patterns with two dominant length scales (~1 μm and ~100 nm). Both of these length scales as well as the film thickness increase linearly with total polymer concentration in the solvent. Phase separation on two length scales is concluded. © 2002 Elsevier Science B.V. All rights reserved.

Keywords: Atomic force microscopy; Friction; Self-assembly; Surface thermodynamics (including phase transitions); Growth

1. Introduction

Surface phase transitions [1] and thermodynamics [2] of thin polymer blend films are of utmost current interest. In many practical applications films of incompatible mixtures are prepared by spin-coating from a common solvent. Phase separation enabled by the solvent added to the polymers (i.e. by a 'solvent quench' into non-stable region of the phase diagram) is rapidly terminated as the solvent evaporates [3–10]. Formed non-equilibrium phase domain structures, accompanied by the undulations at the film surface, are either undesirable or intended (e.g. as in antireflection coatings [6]). Phase separation due to solvent quench has been studied almost exclusively for binary polymer blends [3,5–10]. Important modification of this process was noticed when the third polymer component (surfactant) was added and segregated at the interfaces between the other phases [4]. In this case, as the surfactant reduces the interfacial energy, extended interfaces are formed.

Recently, we have described surface patterns, related with topography and phase morphology, formed in blend films of deuterated polystyrene (dPS) and poly(2-vinylpyridine) (PVP) cast on a substrate modified by hydrophobic self-assembled monolayers (SAM) [5]. Here, our study is extended to a model ternary blend of dPS, PVP and poly-(methyl methacrylate) PMMA [4]. We analyze films with the surface patterns characterized by two well defined length scales where double phase separation is expected [3,11]. We examine

* Corresponding author.
E-mail address: ufbudkow@cyf-kr.edu.pl (A. Budkowski).

PII: S0039-6028(02)01339-0

quantitatively how the characteristic dimensions of phase domains are controlled by the total polymer concentration c_P in a common solvent. We inspect also the relation between surface and bulk phase structure as a function of c_P.

2. Experimental

The polymers used in this work were dPS (molecular weight $M_w = 174$ k, polydisperisty index $M_w/M_n = 1.03$), PVP ($M_w = 115$ k, $M_w/M_n = 1.02$) and PMMA ($M_w = 149$ k, $M_w/M_n = 1.10$), purchased from Polymer Standards Service. Nanometer films (with average thickness $h \sim 30$–90 nm) of ternary blend dPS/PMMA/PVP (with relative weight fractions 2:1:2) were spin-coated at 5800 rpm from tetrahydrofurane (THF) solution with total polymer concentration $c_P = 6$–18 mg/ml onto hydrophobic SAM of hexadecanethiol ($HS(CH_2)_{15}CH_3$) formed on Au-covered silicon wafers [5]. Topography and friction images of the cast thin films were collected simultaneously by atomic (AFM)- and lateral (LFM)-force modes of CP Park Scientific Instruments microscope working in contact mode with a Si_3N_4 cantilevered tip and a typical load of 20 nN. The overall phase domain morphology was determined by AFM examination combined with selective dissolution of PVP and dPS-rich phase for the films immersed for 5 min in ethanol [4,5] and cyclohexane [4], respectively. Film thickness h was determined from AFM images taken after partial removal of the polymer blend film by a scalpel scratch.

3. Results

Three types of data sets were collected in order to probe different characteristics of the blend films. First, topographic and friction surface images were acquired for blends cast with increasing polymer concentration c_P. They are shown in Figs. 1A–B, 1C–D, 1E–F and 2A–B for $c_P = 6$, 7, 9 and 18 mg/ml, respectively. Second, the overall phase domain morphology was revealed by AFM images (depicted here for $c_P = 18$ mg/ml) taken for the films as prepared (Fig. 2A) and after subsequent selective dissolution of PVP- (Fig. 2C) and dPS- (Fig. 2D) rich phases. Finally, film thickness was evaluated from the AFM images of the region with polymer film and bare substrate as represented in Fig. 3A and C for the $c_P = 9$ mg/ml sample.

4. Discussion

An inspection of AFM images (Figs. 1A, C and E and 2A) and related histograms (not shown here) reveals bimodal height distribution and enables us to determine two characteristic topographic levels and average height value. The average film thickness $h = \Delta h_F + \Delta h_S$ was evaluated as the sum of two components. First component Δh_F (marked on Fig. 3E) is defined as the difference between the average height and the lower topographic level of the blend film. The second component Δh_S is measured directly from topographic cross-section taken on the polymer film edge (Fig. 3C) and corresponds to the difference between the lower topographic level of the blend film and the level of the substrate. In this manner the average film thickness was evaluated for *blends* cast with various polymer concentration c_P. The relation $h(c_P)$, depicted in Fig. 4A, follows linear relation predicted [12] and observed [13] for spin-coated films of *pure* polymers. This observation indicates that all complex spin-coating mechanisms (such as centrifugal and viscous forces, polymer diffusion and solvent evaporation [12]) are similar in both cases. It suggests also that surface undulations (characteristic for blend films) are formed during the final stage of spin-coating process when film thickness is modified predominantly by rapid solvent evaporation [7].

As shown in Figs. 1A, C, E and 2A, film surface undulations form well developed patterns with two dominant length scales d_L and d_S: large coarse, essentially elongated elevations (d_L) and much smaller circular protrusions (d_S). Both structures coarsen for increased polymer concentration c_P. To examine this phenomenon more quantitatively we have analyzed AFM images numerically using approach proposed in Refs. [3,5,14]. In this approach d_L can be defined by the wave vector

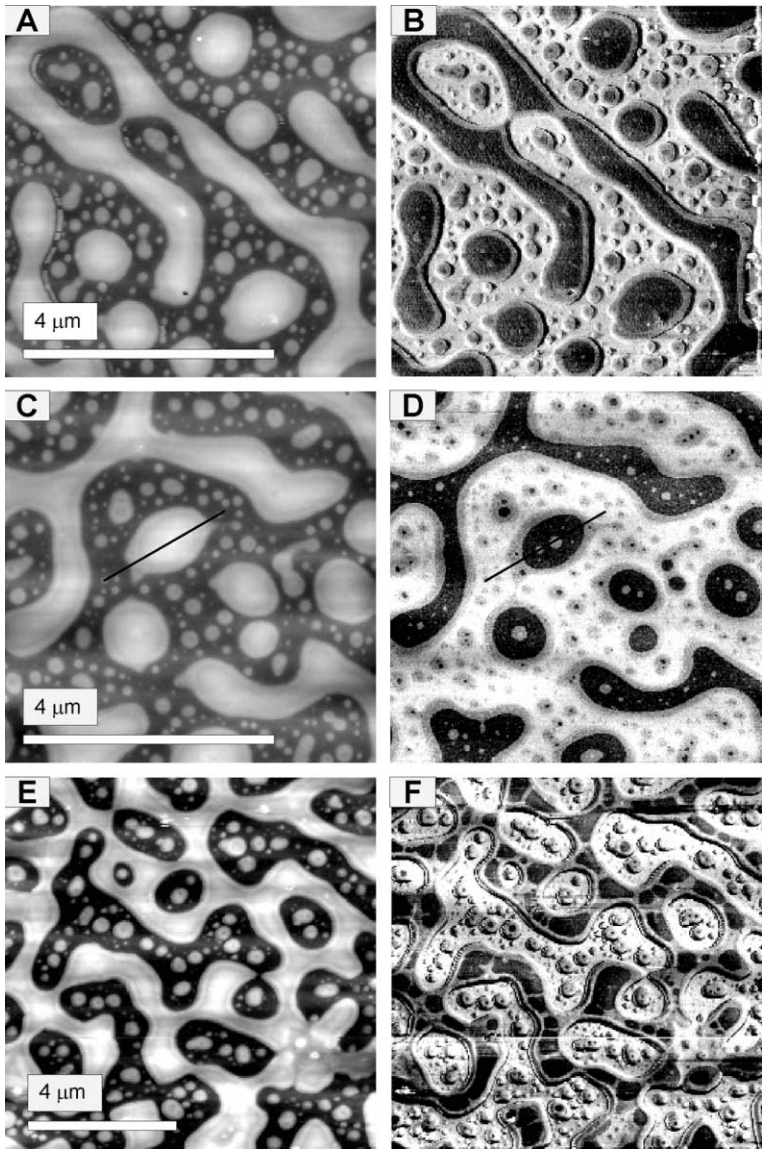

Fig. 1. AFM (A, C, E) and LFM (B, D, F) surface images collected simultaneously for PVP/PMMA/dPS blends cast from THF with polymer concentration $c_P = 6$ (A, B), 7 (C, D) and 9 mg/ml (E, F). The gray level (in this and other figures) depicts the height (AFM)- or LFM signal-scale. White (black) color corresponds to high values on AFM (LFM) pictures.

$k_{max} = 1/d_L$, where k_{max} corresponds to maximum of radial averaged power spectrum of fast Fourier transform calculated for (not presented—80×80 μm^2) AFM images. Parameter d_S is given ($S_S = \pi d_S^2$) by mean area S_S of small circular protrusions determined by integral geometry methods. Determined dependence of d_L and d_S on polymer concentration c_P, shown in Fig. 4B and C, follows a linear relation.

The potential of LFM measurements for the chemical imaging of organic films (SAM monolayers [15], polymer blends [8,9]) has been recognized a few years ago. Here we present first successful application of LFM to determine the

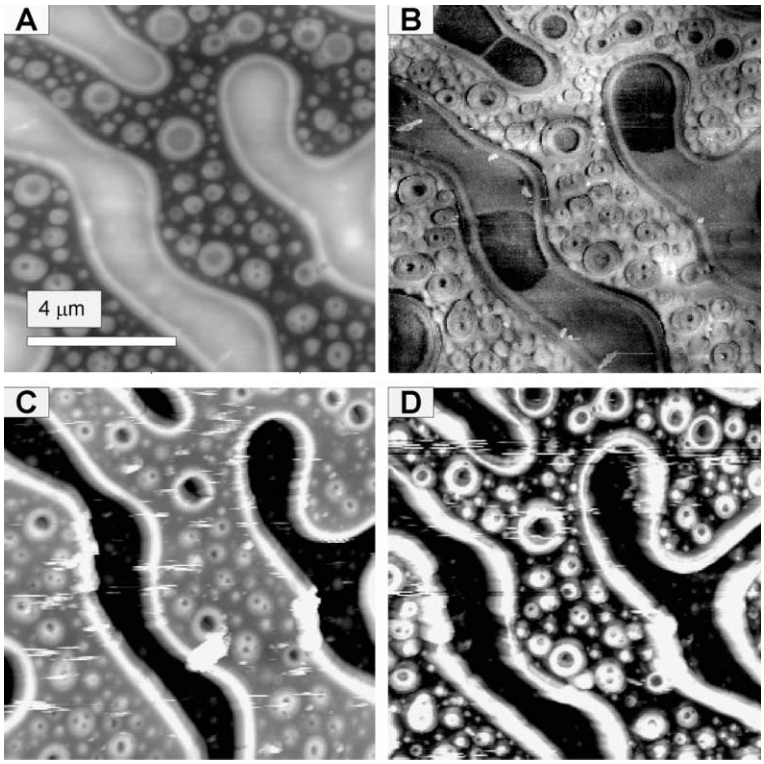

Fig. 2. AFM (A, C, D) and LFM (B) surface images collected for PVP/PMMA/dPS blends cast from THF with total polymer concentration $c_P = 18$ mg/ml prior (A, B) and after subsequent selective dissolution of PVP (C)- and dPS (D)-rich phases.

distribution of surface phase domains in ternary blend films. An inspection of LFM images (Figs. 1B, D, F and 2B) reveals three levels of the lateral force for the blend films (see also LFM cross-sections in Fig. 3D and F). For organic films with similar elastic modulus main contribution to the friction comes from adhesive force between the tip and the studied film region characterized by surface tension γ [8,9,15]. Since for a polar (Si_3N_4) tip LFM signal increases with γ [8,9,15] and γ(dPS) $<$ γ(PMMA) [10] $<$ γ(PVP) [16], we attribute successive LFM signal levels (Fig. 3D and F) to dPS, PMMA and PVP. Accordingly white, gray and black color on LFM images (Figs. 1 and 2) correspond to dPS, PMMA and PVP.

Now we are ready to discuss surface phase domain morphology and its relation with surface topography. We start by noting that (white) dPS- and (black) PVP-rich surface regions of LFM images (Figs. 1B, D, F and 2B) are always separated by PMMA (gray) inclusions. Such behavior reflects the surfactant role played by PMMA which is driven by the balance of three enthalpic interaction parameters (with $\chi_{dPS/PVP} \gg \chi_{PMMA/dPS}$, $\chi_{PMMA/PVP}$ [4]). The comparison of AFM and LFM images (Figs. 1 and 2A, B) reveals also that the elevated film regions correspond to domains rich in PVP and PMMA, while the lower part of the film is composed with dPS-rich phase (cf. Fig. 3C, E and D, F). Such behavior was explained earlier [4] by different rates of solvent evaporation from various polymers. Briefly, PVP and PMMA solidify earlier than dPS which, as a better dissolved polymer, is depleted of the solvent later and, therefore, collapses below the level of the other phase domains.

Careful analysis of friction images reveals that at low polymer concentration c_P the surface phase rich in PMMA (gray) was located mainly at the edges of large coarse elevations (Fig. 1B and D).

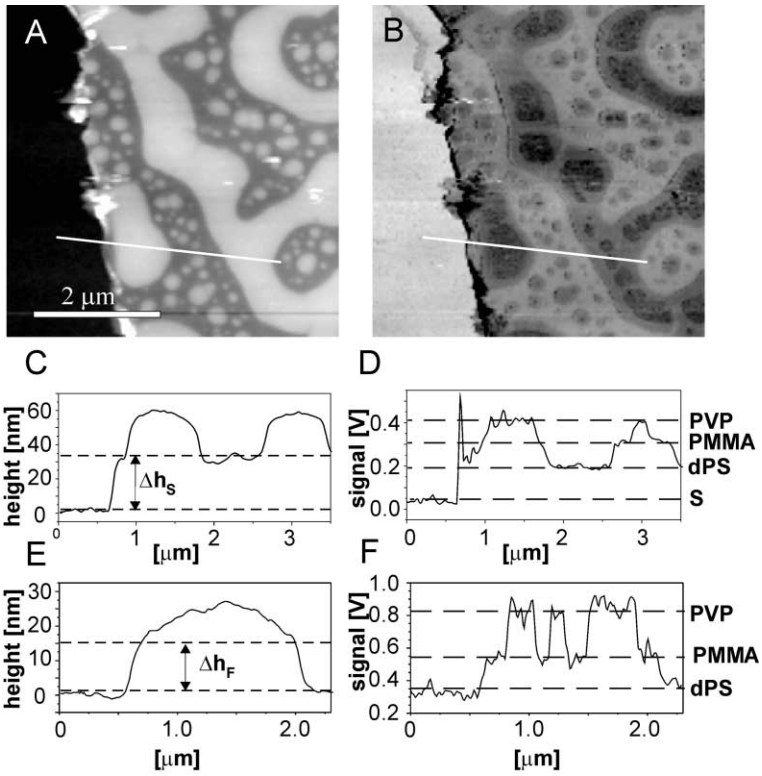

Fig. 3. AFM (A) and LFM (B) image of the sample region with the blend film ($c_P = 9$ mg/ml) and with bare substrate. The line in the images A and B indicates the location where AFM (C)- and LFM (D)-cross-sections were taken. AFM (E) and LFM (F)-cross-sections of the $c_P = 7$ mg/ml film were taken along the lines shown in Fig. 1C and D. The height difference between the lower topographic level in the blend film and the substrate level (Δh_S) is marked in C. The height difference between the lower topographic level and the average height (Δh_F) in the blend film is marked in E. LFM signal levels corresponding to PVP, PMMA, dPS and the substrate (s) are represented by dashed lines in D and F.

With increasing c_P this phase progressively covers inner regions of the elevations (Figs. 1F and 2B) which were earlier occupied almost exclusively by the PVP-rich phase (black). To investigate the correspondence between these and other surface and bulk features of the phase domain morphology, we compare now LFM data (Fig. 2B) with AFM results obtained prior (Fig. 2A) and after subsequent selective dissolution of PVP (Fig. 2C) and dPS (Fig. 2D). This comparison (performed for the $c_P = 18$ mg/ml sample) confirms the concluded earlier relation between LFM signal level and various surface phases. It shows also that the coverage of the inner regions of large coarse elevations by PMMA-rich phase is merely a surface effect.

5. Summary and conclusions

The domains of ternary blend dPS/PMMA/PVP films, phase-separated in the course of spin-coating from a common solvent, form quasi-two-dimensional structures with dPS- and PVP-rich domains separated by PMMA inclusions. In addition, for increasing total polymer concentration c_P, the PVP-rich bulk domains are observed to become progressively covered by surface layers rich in PMMA. Surface topography and phase domain morphology are closely related. Lower surface regions correspond to dPS-rich domains while elevated areas to phases rich in PVP and PMMA. Topographic structures with two dominant length scales ($d_L \sim 1$ μm, $d_S \sim 100$ nm) are

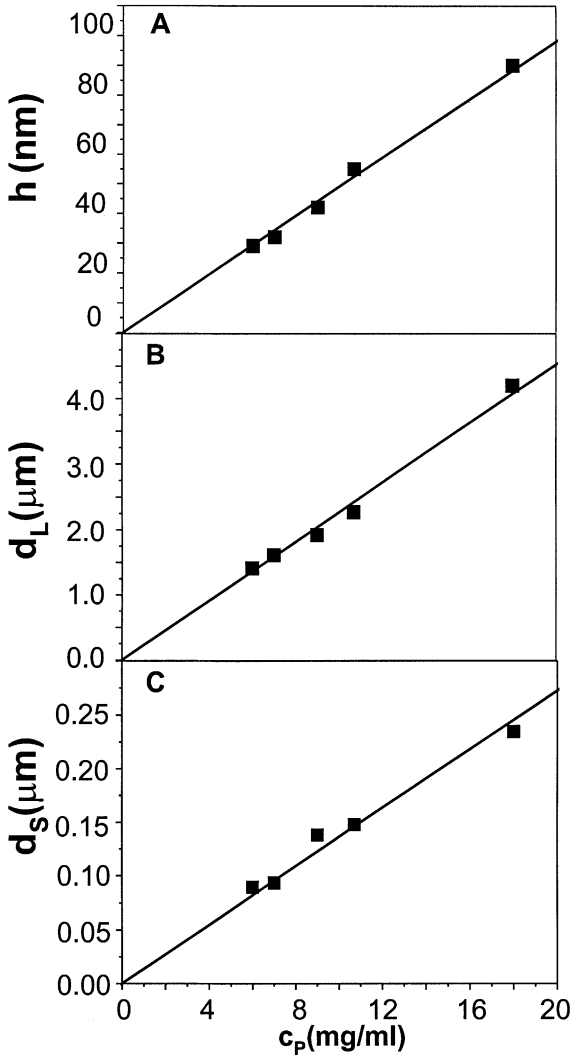

Fig. 4. Average polymer film thickness h (A) and two characteristic length scales: d_L (B) and d_S (C) of surface undulations plotted as a function of total polymer concentration c_P. Solid lines indicate one-parameter linear fit.

formed. Both d_L and d_S as well as average film thickness h of the blend film grows linearly with c_P.

Our results indicate that observed two types of topographic structures correspond to bimodal distribution of phase domains and originate from phase separation on two length scales (not observed in the absence of surfactant blend component (PMMA) for analogous blend PVP/dPS [5]). Most probably the large-scale formation of domain structure (with phase compositions far from equilibrium values) is driven by fast hydrodynamic process [11]. Smaller circular domains are formed most likely due to secondary phase separation [11] in macroscopically separated dPS-rich domains, where solvent is depleted later and polymers are mobile longer. Observed relation between average film thickness (controlled by c_P) and the length scales of both domain structures can be explained assuming that in thicker films the solvent is present longer, allowing for a longer period of polymer mobility and, hence, higher degree of phase domain coarsening during the spin-coating process [7].

Acknowledgements

This work was supported by Grants of the Institute of Physics, by Reserve of the Rector of the Jagiellonian University, by Polish Committee of Scientific Research, M. Sklodowska-Curie Foundation and by NATO grant. The authors also thank Professor M. Szymoński for the access to the AFM/LFM microscope at Regional Laboratory for Physical and Chemical Analysis of the Jagiellonian University.

References

[1] J. Rysz, A. Budkowski, A. Bernasik, J. Klein, K. Kowalski, J. Jedlinski, L.J. Fetters, Europhys. Lett. 50 (2000) 35; Europhys. Lett. 43 (1998) 404.
[2] G. Krausch, Mater. Sci. Eng. R 14 (1995) 1; K. Binder, Adv. Polymer Sci. 138 (1999) 1; A. Budkowski, Adv. Polymer Sci. 148 (1999) 1.
[3] J.S. Gutmann, P. Müller-Buschbaum, M. Stamm, Faraday Discuss. 112 (1999) 285.
[4] S. Walheim, M. Ramstein, U. Steiner, Langmuir 15 (1999) 4828.
[5] P. Cyganik, A. Bernasik, A. Budkowski, B. Bergues, K. Kowalski, J. Rysz, J. Lekki, M. Lekka, Z. Postawa, Vacuum 63 (2001) 307; Vacuum 63 (2001) 297.
[6] S. Walheim, E. Schaffer, J. Mlynek, U. Steiner, Science 283 (1999) 520.
[7] S. Walheim, M. Böltau, J. Mlynek, G. Krausch, U. Steiner, Macromolecules 30 (1997) 4995.
[8] G. Krausch, M. Hipp, M. Böltau, O. Marti, J. Mlynek, Macromolecules 28 (1995) 260.

[9] K. Feldman, T. Tervoort, P. Smith, N.D. Spencer, Langmuir 14 (1998) 372.
[10] K. Tanaka, A. Takahara, T. Kajiyama, Macromolecules 29 (1996) 2229.
[11] H. Tanaka, Phys. Rev. E 51 (1995) 1313.
[12] C.J. Lawrence, Phys. Fluids 31 (1988) 2786.
[13] C. Ton-That, A.G. Shard, R.H. Bradley, Langmuir 16 (2000) 2281.
[14] J. Raczkowska, J. Rysz, A. Budkowski, in preparation.
[15] J.L. Wildbur, H.A. Biebuyck, J.C. MacDonald, G. Whitesides, Langmuir 11 (1995) 825.
[16] C.J. Clarke, A. Eisenberg, J. La Scala, M.H. Rafailovich, J. Sokolov, Z. Li, S. Qu, D. Nguyen, S.A. Schwartz, Y. Strzhemechny, B.B. Sauer, Macromolecules 30 (1997) 4184.